

Direct Extension of Density-Matrix Renormalization Group toward 2-Dimensional Quantum Lattice Systems: Studies for Parallel Algorithm, Accuracy, and Performance

S. Yamada,^{*} M. Okumura,[†] and M. Machida[‡]

CCSE, Japan Atomic Energy Agency, 6-9-3 Higashi-Ueno, Taito-ku Tokyo 110-0015, Japan and CREST(JST), 4-1-8 Honcho, Kawaguchi, Saitama 332-0012, Japan

(Dated: December 24, 2021)

We parallelize density-matrix renormalization group to directly extend it to 2-dimensional (n -leg) quantum lattice models. The parallelization is made mainly on the exact diagonalization for the superblock Hamiltonian since the part requires an enormous memory space as the leg number n increases. The superblock Hamiltonian is divided into three parts, and the correspondent superblock vector is transformed into a matrix, whose elements are uniformly distributed into processors. The parallel efficiency shows a high rate as the number of the states kept m increases, and the eigenvalue converges within only a few sweeps in contrast to the multichain algorithm.

PACS numbers: 71.10.Fd, 71.10.Pm, 74.20.Mn, 03.75.Ss

The superfluidity achieved in atomic Fermi gas [1] is quite useful in studying strongly-coupled superfluidity. Very recently, such a success has intensively pushed experimentalists to find another type of superfluidity, which emerges on strongly-correlated 2-dimensional (2-D) lattice system. This is because the so-called “optical lattice” build in atomic gases may offer a testbed to directly solve the Hubbard model and related controversial issues in High- T_c cuprate superconductors in a controllable manner [2].

So far, several computational approaches have been proposed in order to study strongly-correlated lattice fermions. Among them, three methods, i.e., the exact-diagonalization, the density-matrix renormalization group (DMRG) [3, 4], and the quantum Monte Carlo are widely employed as standard and established ones. However, 2-D systems are too complicated for these methods to uncover, and the ground-states in the most 2-D models are still open problems. In this paper, we therefore suggest a parallel algorithm to directly extend DMRG to 2-D models.

The DMRG method, which was originally aimed for 1-D lattice model, can be extended to 2-D models (n -leg models) as depicted in Fig. 1 (a). Then, the number of the states required in the direct algorithm is roughly given as $16^s m^2$ ($4^s m^2$) for s -leg Hubbard model (the s -leg Heisenberg model) per block, in which m is the number of states kept. Although the degree of freedom practically decreases with eliminating irrelevant states, it is clear that a slight increment of the leg gives rise to an exponential like growth of the state number. Thus, the direct extension has been limited within 2-leg [5], and the previous 2-D DMRG has adopted the so-called multichain algorithm as depicted in Fig. 1 (b) since its memory space is basically comparable to the 1-D case [4]. However, the

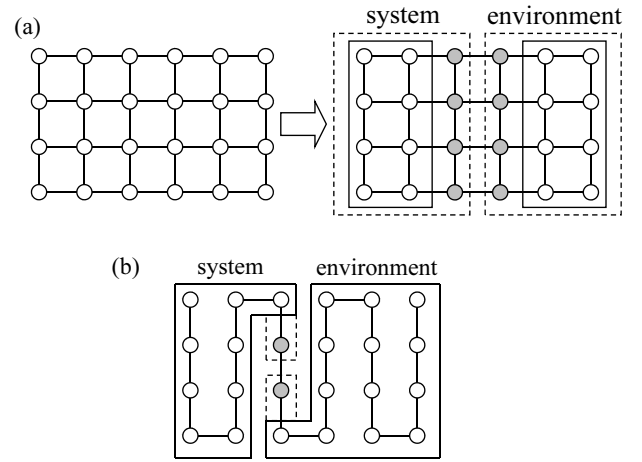


FIG. 1: (a) A superblock configuration to directly perform DMRG for 2-D lattice models. (b) The conventional configuration using “multichain” algorithm to avoid enormous memory expansion.

multichain algorithm has difficulties in its convergence property and accuracy [4, 6].

The direct 2-D extension of DMRG guarantees high accuracy similar to 1-D cases, although it requires an enormous memory space. Thus, if possible, it is valuable to parallelize the direct 2-D DMRG and obtain a scalable code, which enables to raise the number of legs with increasing computational resources. The present-day big supercomputers have a tera-byte order of memory. We therefore claim that a scalable algorithm may be crucial in advancing computational research on 2-D models. We examine the parallel efficiency as well as the convergence property of 2-D direct DMRG on a parallel supercomputer Altix 3700Bx2 in JAEA.

Let us explain the parallel algorithm. In the direct 2-D DMRG as shown in Fig. 1 (a), a routine which consumes most of the computer resources, i.e., memory and CPU time, is the exact diagonalization of the superblock Hamiltonian H . Inside the routine, a major operation is

^{*}Electronic address: yamada.susumu@jaea.go.jp

[†]Electronic address: okumura.masahiko@jaea.go.jp

[‡]Electronic address: machida.masahiko@jaea.go.jp

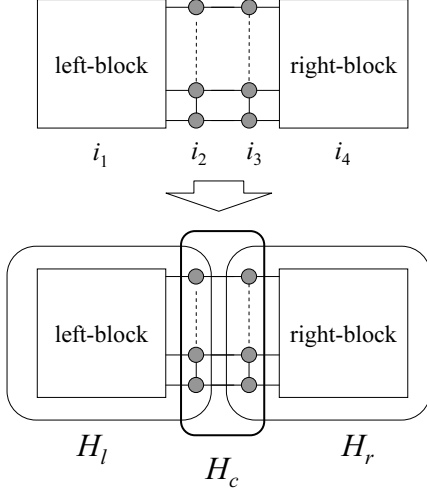


FIG. 2: A superblock of 2-D direct DMRG, which is composed of four blocks named “block 1”, “block 2”, “block 3”, and “block 4” from the left. See the text for the index i_j (top panel). H_l , H_r , and H_c (bottom panel) denote the decomposed block Hamiltonians in the left, the right, and the central block, respectively.

the multiplication between the Hamiltonian matrix and the vector, i.e., Hv . This is the most basic operation repeated over and over again in the exact diagonalization and DMRG. In general, the parallelization of the multiplication between the sparse Hamiltonian matrix [7] and the vector can be simply realized by distributing the sparse matrix rowwisely. However, it is difficult to obtain a good load balance for the cases like the interacting 2-D lattice fermions, whose non-zero element distribution is not so regular. In this paper, we, therefore, propose an alternative parallel strategy, which transforms the superblock vector into a matrix form, and distribute the matrix into processors.

Let us write down the algorithm. Each block of the superblock is called “block 1”, “block 2”, “block 3”, and “block 4” from the left, and the state of the “block j ” is represented as i_j (see the top panel of Fig. 2). Then, the Hamiltonian matrix $H_{i_1 i_2 i_3 i_4; i'_1 i'_2 i'_3 i'_4} (= H)$ is given by

$$\begin{aligned} H_{i_1 i_2 i_3 i_4; i'_1 i'_2 i'_3 i'_4} &= H_{i_1 i_2; i'_1 i'_2} \delta_{i_3 i_4; i'_3 i'_4} + H_{i_3 i_4; i'_3 i'_4} \delta_{i_1 i_2; i'_1 i'_2} \\ &+ H_{i_2 i_3; i'_2 i'_3} \delta_{i_1 i_4; i'_1 i'_4}, \end{aligned} \quad (1)$$

where $\delta_{i,j}$ is the Kronecker’s delta, and $H_{i_1 i_2; i'_1 i'_2}$, $H_{i_3 i_4; i'_3 i'_4}$, and $H_{i_2 i_3; i'_2 i'_3}$ are the block Hamiltonian matrices in the left block, the right block, and the central block, respectively. In the following, we express them as H_l , H_r , and H_c (see the bottom panel of Fig. 2) for simplicity. Here, we put the $((i_3 - 1)m^2n + (i_4 - 1)mn + (i_2 - 1)m + i_1)$ -th element of the vector v , which corresponds to the state $|i_1 i_2 i_3 i_4\rangle$, into an element $((i_2 - 1)m + i_1, (i_3 - 1)m + i_4)$ of a matrix V . Then, the multiplication $H_l \delta_{i_3 i_4; i'_3 i'_4} v$ and $H_r \delta_{i_1 i_2; i'_1 i'_2} v$ are rewritten

as the following matrix-matrix multiplications

$$\begin{aligned} H_l \delta_{i_3 i_4; i'_3 i'_4} v &\mapsto H_l V, \\ H_r \delta_{i_1 i_2; i'_1 i'_2} v &\mapsto V H_r^T, \end{aligned}$$

where H^T denotes the transpose of H . Similarly, when the same element is put into the element $((i_3 - 1)n + i_2, (i_4 - 1)m + i_1)$ of another matrix V_c , the multiplication $H_c v$ is rewritten into

$$H_c \delta_{i_1 i_4; i'_1 i'_4} v \mapsto H_c V_c.$$

While the matrix H_l , H_r , and H_c are sparse matrices, the matrices V and V_c are complete dense ones since these are formed by elements of the superblock vector v . This indicates that the parallel calculation for the matrix-vector multiplication Hv can be effectively executed by partitioning the matrices V and V_c . This parallelization scheme has been successfully employed in the exact diagonalization. The details of the parallel scheme and efficiency were reported in [8, 9]. By using this algorithm, one can extend DMRG to arbitrary n -leg model as long as computation resources are unlimited. In addition, the direct method has several advantages. The application of the periodic boundary condition is not a problem at all, and the extension to the time-dependent, the dynamical, and the finite temperature DMRG [4] is straightforward. However, it should be noted that the increment of the ladder leg enlarges not only the dimension of the Hamiltonian matrix but also that of the density matrix. Although the size of the density matrix becomes not so large, its diagonalization needs m eigenstates and its CPU time cost becomes non-negligible with the leg increment. The parallelization in terms of the density matrix is another difficult issue, since the size of the block diagonal matrices inside the density matrix can not be predicted prior to the execution. The parallelization should be adaptive to the dynamical change of the size. Its algorithm and technique will be published elsewhere [10]. In this paper, we restrict ourselves within the parallelization for the Hamiltonian matrix operation, since it is the most primary issue for 2-D extension. The maximum leg sizes in this paper are 9 (its results are not shown) and 5 for Heisenberg and Hubbard model, respectively, due to the limitation of CPU resource [11].

Let us present calculation results of the direct DMRG. Figure 3 (a) and (b) show how the ground state energy converges with repeating the sweep for $5(\text{leg}) \times 10$ -site Heisenberg model ($J_z = J_{xy} = 1$) and the 3×10 -site Hubbard model ($U/t = 10$) with 28 fermions ($14 \uparrow, 14 \downarrow$). The open boundary condition is applied to both models. These results demonstrate that both models converge to their ground state within once or twice sweeps [12]. Moreover, the ground state energy sufficiently converges with $m \sim 128$ and ~ 256 for Heisenberg and Hubbard model, respectively. These features clearly prove that the direct DMRG method is quite excellent in the accuracy and the convergence properties in contrast to the multichain algorithm [6].

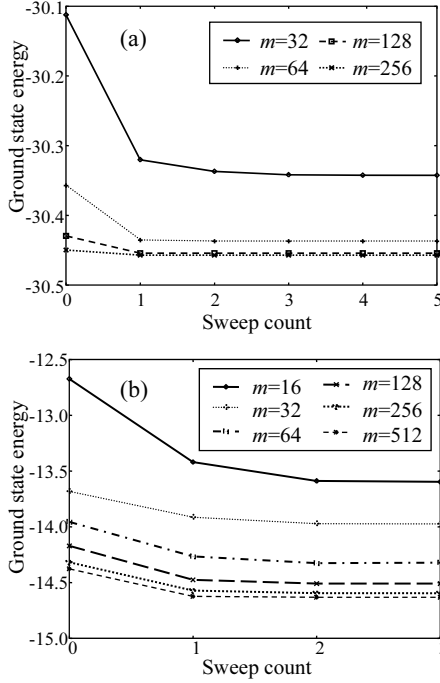


FIG. 3:

The ground state energy vs. the sweep counts for (a) $5(\text{leg}) \times 10$ -site Heisenberg model and (b) 3×10 -site Hubbard model. m is the number of states kept.

Next, we present the performance of the direct DMRG method. A test example is the two-dimensional 7×10 -site Heisenberg model. Fig. 4 (a) shows how CPU time decreases with increasing CPU number, and how the parallel scalability depends on m . The latter effect is comprehensible through a comparison among $m = 32, 64$, and 128 . It is clear that the parallelization effect is improved when the number of states kept m increases. This is because the size of the Hamiltonian matrix to be diagonalized grows with m , and the parallelized operation counts increases. This behavior is common for 4×10 -site Hubbard model with 38 fermions ($19 \uparrow, 19 \downarrow$) as shown in Fig. 4 (b). Thus, the direct 2D DMRG is a suitable application for parallel computer, since the true ground-state exploration requires sufficiently large m .

Let us analyze details of the performance of the parallel direct DMRG to discuss the feasibility of the present algorithm for larger m and leg systems. Figure 5 (a) shows how CPU time of three main routines enlarges with increasing m . The three routines are the density matrix formation (DMF), the density matrix diagonalization (DMD), and the Hamiltonian matrix exact-diagonalization (HMED). The target model is 3-leg Hubbard model and 128 CPU's are used in all cases for a comparison. One notices that the cost of HMED especially grows with increasing m . If HMED is not parallelized, then CPU cost for HMED is found to be too huge. The parallelization for HMED is clearly crucial. Fig. 5 (b) is a leg number dependence of CPU time balance for the

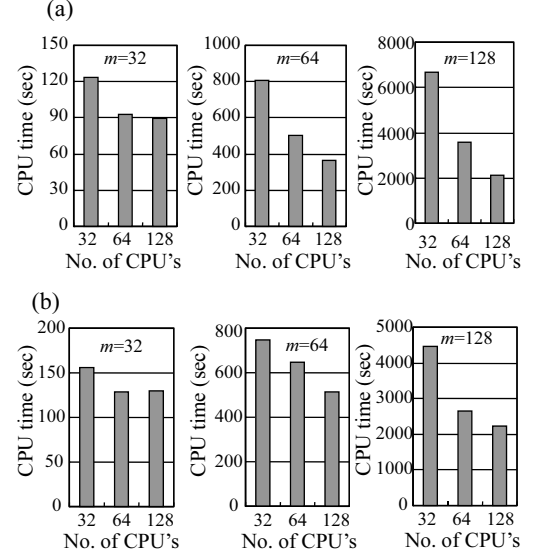


FIG. 4: The CPU number dependence of the total CPU time for (a) $7(\text{leg}) \times 10$ -site Heisenberg model on Altix3700Bx2 with $m = 32, 64$, and 128 . (b) The same dependence for 4×10 Hubbard model.

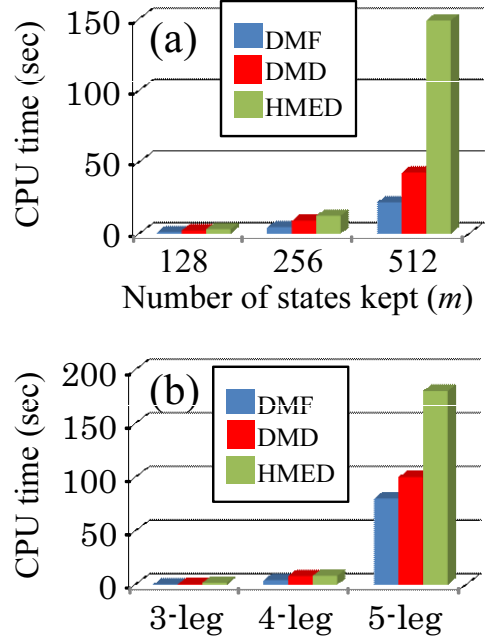


FIG. 5: (a) The m dependence of CPU cost distribution for three main routines (see the text) of the present DMRG code. The model is 3 (leg) \times 10-site Hubbard model. CPU time of each routine is averaged per step of DMRG. For every case, 128 CPU's on Altix3700Bx2 are used. (b) The leg number dependence of CPU cost distribution for the Hubbard model. In all cases, $m = 64$, and 128 CPU's are used.

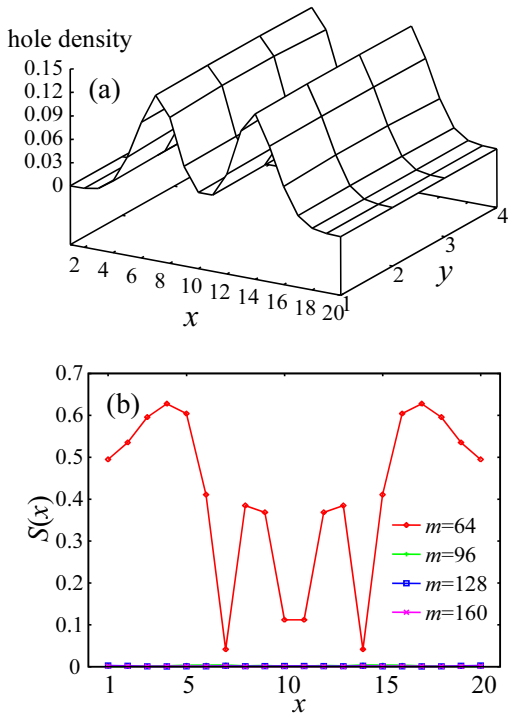


FIG. 6: (a) The hole density profile for 4(leg) \times 20-site Hubbard model ($U/t = 10$) with 76 fermions ($38 \uparrow$, $38 \downarrow$) and $m = 160$. (b) The ladder direction dependence of the maximum value of the local staggered spin density along the leg direction for the same model with $m = 64, 96, 128$, and 160 .

three routines with $m = 64$. Although HMED sustains the position as the heaviest routine on the increment of the leg number, it is noted that the sum of DMF and DMD is comparable to HMED for 5-leg model. These results indicate that CPU costs in terms of the density matrix also becomes a bottleneck for larger leg cases.

Finally, let us examine the validity of the ground state obtained by the present direct DMRG. We pay attention to the Hubbard model with just below the half-filling. The reason is that there is a controversial issue whether the stripe is the ground state or not [13]. We calculate spatial profiles of the hole density

$$h(x, y) = 1 - \langle \hat{n}_{x,y,\uparrow} + \hat{n}_{x,y,\downarrow} \rangle, \quad (2)$$

and the staggered spin density

$$s(x, y) = \langle \hat{n}_{x,y,\uparrow} - \hat{n}_{x,y,\downarrow} \rangle, \quad (3)$$

with an open boundary condition for each direction. Here, $\hat{n}_{x,y,\sigma}$ ($\sigma = \uparrow, \downarrow$) is the density operator and $\langle \cdots \rangle$

denotes the ground state expectation value. One expects $s(x, y) = 0$ for any local sites in the ground state of the finite ladder Hubbard model, even if the hole density modulation survives. This is a consequence of Lieb-Mattis theorem [6, 14]. We calculate the ground state profiles of the 4×20 -site Hubbard model with 76 spins ($38 \uparrow$, $38 \downarrow$) at $U/t = 10$ with varying from $m = 64$ to $m = 160$. Figure 6 (a) shows the hole density profile for $m = 160$, while Fig. 6(b) presents m dependence of the ladder direction profiles of the maximum value of the staggered spin density along the leg-direction given as

$$S(x) = \max_{y=1}^4 |s(x, y)|. \quad (4)$$

We point out that the present DMRG method rapidly converges non-polarized pattern for the staggered spin density profile with increasing m , although the hole density one shows a stripe structure. These results are different from those of the multichain algorithm [6], in which an extrapolation is required to remove the artificial profile of the spin density. To our knowledge, such a direct convergence is the first result in DMRG calculation of the 2-D Hubbard model.

We developed a 2-D directly-extended code of DMRG. We parallelized the exact diagonalization part by transforming the superblock vector into the matrix and distributing the elements. This parallel scheme becomes more effective as the number of states kept m increases. In addition, we confirmed in the repulsive 2-D Hubbard model that the stripe observable in the hole density profile is not artificial because the spin-density modulation as its counterpart disappears with increasing m according to Lieb-Mattis theorem. We believe that the present direct 2-D DMRG will give a great impact on the ground state exploration in atomic gas, solid state, and other systems, by the future use of advanced parallel computers.

Two of authors (S.Y. and M.M.) acknowledge M. Kohno, T. Hotta, and H. Onishi for illuminating discussion about the DMRG techniques. M.M. also thanks Y. Ohashi and H. Matsumoto for the Hubbard model. The work was partially supported by Grant-in-Aid for Scientific Research on Priority Area "Physics of new quantum phases in superclean materials" (Grant No. 18043022) from the Ministry of Education, Culture, Sports, Science and Technology of Japan. This work was also supported by Grant-in-Aid for Scientific Research from MEXT, Japan (Grant No.18500033).

[1] C. A. Regal, M. Greiner, and D. S. Jin, Phys. Rev. Lett. **92**, 040403 (2004); T. Bourdel *et al.*, *ibid.* **93**, 050401 (2004); C. Chin *et al.*, Science **305**, 1128 (2004); J. Ki-

nast *et al.*, *ibid.* **307**, 1296 (2005); M. W. Zwierlein *et al.*, Nature (London) **435**, 1047 (2005), and references therein.

- [2] For a review, see, e.g., D. Jaksch and P. Zoller, *Ann. Phys.* **315**, 52 (2005).
- [3] S. R. White, *Phys. Rev. Lett.* **69**, 2863 (1992); *Phys. Rev. B* **48**, 10345 (1993).
- [4] For recent reviews, see e.g., U. Schollwöck, *Rev. Mod. Phys.* **77**, 259 (2005); K. A. Hallberg, *Adv. Phys.* **55**, 477 (2006), and references therein.
- [5] R. M. Noack, S. R. White, and D. J. Scalapino, e-print arXiv:cond-mat/9404100.
- [6] G. Hager, G. Wellein, E. Jackemann, and H. Fehske, *Phys. Rev. B*, **71**, 075108 (2005).
- [7] Generally, the block Hamiltonian matrix becomes sparse in 2-D models, while it is not so in 1-D models.
- [8] S. Yamada, T. Imamura, and M. Machida, *Proc. of SC05* (2005).
<http://sc05.supercomputing.org/schedule/pdf/pap188.pdf>.
- [9] S. Yamada, T. Imamura, T. Kano, and M. Machida, *Proc. of SC06* (2006).
<http://sc06.supercomputing.org/schedule/pdf/gb113.pdf>.
- [10] In preparation.
- [11] We set 3 hours execution using 128CPU's on Altix3700 Bx2 as a resource limitation in this paper.
- [12] For smaller ladder cases, e.g, 3×6 Hubbard model, we confirm that the converged eigenvalue shows an almost perfect agreement with that of the exact-diagonalization.
- [13] D. J. Scalapino, e-print arXiv:cond-mat/0610710.
- [14] S. R. White and D. J. Scalapino, *Phys. Rev. Lett.* **91**, 136403 (2003).